Kinetics of Ca^{2+}-Induced Fusion of Cardiolipin–Phosphatidylcholine Vesicles: Correlation between Vesicle Aggregation, Bilayer Destabilization, and Fusion†

Jan Wilschut,*,‡ Shlomo Nir,§ Janny Scholma,‡ and Dick Hoekstra‡

Laboratory of Physiological Chemistry, University of Groningen, Bloemsingel 10, 9712 KZ Groningen, The Netherlands, and Seagram Center for Soil and Water Sciences, Faculty of Agriculture, The Hebrew University of Jerusalem, Rehovot 76100, Israel

Received October 2, 1984; Revised Manuscript Received February 25, 1985

ABSTRACT: We have investigated the kinetics of Ca^{2+}-induced aggregation and fusion of large unilamellar vesicles composed of an equimolar mixture of bovine heart cardiolipin and dioleoylphosphatidylcholine. Mixing of bilayer lipids was monitored with an assay based on resonance energy transfer (RET) and mixing of aqueous vesicle contents with the Tb/dipicolinate assay. The results obtained with either assay were analyzed in terms of a mass action kinetic model, providing separate rate constants for vesicle aggregation and for the fusion reaction proper. At different Ca^{2+} concentrations, either at 25 °C or at 37 °C, aggregation rate constants derived from the data obtained with the RET assay were the same as those derived from the Tb/dipicolinate data, indicating that mixing of bilayer lipids occurred only during vesicle aggregation events that resulted in mixing of aqueous contents as well. At 25 °C, identical fusion rate constants were obtained with either assay, indicating that at this temperature the probability of lipid mixing and that of aqueous contents mixing, occurring after vesicle aggregation, were the same. The fusion rate constants for the RET assay increased more steeply with increasing temperature than the fusion rate constants derived from the Tb/dipicolinate data. As a result, at 37 °C the tendency of the vesicles, after aggregation, to mix lipids was slightly higher than their tendency to mix aqueous contents. The aggregation rate constants increased steeply with Ca^{2+} concentrations increasing in a narrow range (9.5–11 mM), indicating that, in addition to a Ca^{2+}-dependent charge neutralization on the vesicle surface, structural changes in the lipid bilayer are involved in the aggregation process. Since the fusion rate constants increased remarkably in parallel with the aggregation rate constants, it is concluded that the structural changes in the vesicle bilayer, that facilitate vesicle aggregation, also cause a destabilization of the bilayer and, thus, render the vesicles susceptible to fusion.

The divalent cation induced interaction between negatively charged phospholipid vesicles has been studied extensively as a model for biological membrane fusion [for reviews, see Papahadjopoulos et al. (1979), Nir et al. (1983), and Wilschut & Hoekstra (1984)]. Thus, the general characteristics of Ca^{2+}-induced fusion of vesicles containing phosphatidylserine (PS)[1] (Papahadjopoulos et al., 1977; Portis et al., 1979; Wilschut et al., 1980, 1981, 1983; Hoekstra, 1982; Düzgünes et al., 1981a,b, 1984), cardiolipin (CL) (Wilschut et al., 1982), or other acidic phospholipids (Sundler & Papahadjopoulos, 1981; Sundler et al., 1981) have been elucidated. However, despite a wealth of knowledge on these systems is available now, the detailed molecular mechanism of phospholipid vesicle fusion remains largely obscure, as yet.

Phospholipid vesicles, in general, are very stable structures that do not normally fuse spontaneously. As for negatively charged vesicles, long-range electrostatic repulsion prevents vesicle aggregation and fusion. Divalent cations, by binding to negatively charged phospholipid vesicles, reduce electrostatic repulsion and, thus, induce vesicle aggregation (Portis et al., 1979; Papahadjopoulos et al., 1977). However, aggregation in itself is not a sufficient condition for induction of bilayer fusion. For example, Mg^{2+} induces massive aggregation of PS large unilamellar vesicles (LUV), but fusion does not occur (Wilschut et al., 1981), indicating that yet another barrier has to be overcome in order for aggregated vesicles to fuse. It seems likely that this barrier is due to strong repulsive hydration forces that prevent hydrophobic interaction between phospholipid bilayers at short distances of separation [for a review, see Rand (1981)]. Fusion requires the disruption of this hydration barrier, which obviously must involve the occurrence of structural changes in the vesicle bilayer.

In a previous paper, we have demonstrated that fusion of LUV, composed of an equimolar mixture of cardiolipin and phosphatidylcholine, requires a minimal Ca^{2+} concentration in the medium of approximately 9 mM. At Ca^{2+} concentrations below this threshold value, the vesicles neither aggregate nor release encapsulated solutes (Wilschut et al., 1982). In the present study, we performed a detailed kinetic characterization of the fusion of CL/DOPC LUV at different Ca^{2+} concentrations, utilizing the Tb/dipicolinic acid (Tb/DPA) assay (Wilschut & Papahadjopoulos, 1979; Wilschut et al., 1980, 1981, 1983) to monitor the mixing of aqueous vesicle contents and the resonance energy transfer (RET) assay described by Struck et al. (1981) to monitor the mixing of bilayer lipids. By analyzing the results in terms of a mass action kinetic model (Nir et al., 1982, 1983; Bentz et al., 1983a,b),

† This study was supported in part by the Netherlands Organization for the Advancement of Pure Research (Z.W.O.), The Hebrew University of Jerusalem (Shainbrun Funds), NATO (Research Grant 151.81), and EMBO (short-term fellowship to S.N.).

‡ University of Groningen.

§ The Hebrew University of Jerusalem.

[1] Abbreviations: CL, cardiolipin (bovine heart); DPA, dipicolinic acid; DOPC, L-α-dioleoylphosphatidylcholine; Hepes, *N*-(2-hydroxyethyl)-piperazine-*N*′-2-ethanesulfonic acid; LUV, large unilamellar vesicles; *N*-NBD-PE, *N*-(7-nitro-2,1,3-benzoxadiazol-4-yl)phosphatidylethanolamine; *N*-Rh-PE, *N*-(lissamine Rhodamine B sulfonyl)phosphatidylethanolamine; PS, phosphatidylserine; RET, resonance energy transfer; EDTA, ethylenediaminetetraacetic acid.

0006-2960/85/0424-4630$01.50/0

we have determined separately the rate constants for vesicle aggregation and for the fusion reaction per se. It is concluded that, in a Ca^{2+} concentration range just above the threshold of 9 mM, structural changes occur in the vesicle bilayer. These structural changes, that are presumably induced by vesicle/vesicle interaction, facilitate vesicle aggregation and at the same time destabilize the bilayer, thus rendering the vesicles susceptible to fusion.

Materials and Methods

Materials. Bovine heart cardiolipin (CL), L-α-dioleoylphosphatidylcholine (DOPC), *N*-(7-nitro-2,1,3-benzoxadiazol-4-yl)phosphatidylethanolamine (*N*-NBD-PE), and *N*-(lissamine Rhodamine B sulfonyl)phosphatidylethanolamine (*N*-Rh-PE) were obtained from Avanti Polar Lipids, Inc. (Birmingham, AL). $TbCl_3 \cdot 6H_2O$ was from Aldrich (Brussels) and dipicolinic acid (DPA) from Sigma Chemical Co. (St. Louis, MO). All other reagents were of the highest purity available.

Vesicle Preparation. Large unilamellar vesicles (LUV) were prepared from an equimolar mixture of CL and DOPC (lipid phosphorus ratio 2:1) by reverse-phase evaporation (Szoka & Papahadjopoulos, 1978) and successive extrusion (Olson et al., 1979) through 0.2- and 0.1-μm Unipore polycarbonate membranes (Bio-Rad, Richmond, CA), essentially as described before (Wilschut et al., 1980, 1983).

Vesicles to be used in the Tb/DPA assay were prepared in one of the following aqueous media: (i) 5 mM $TbCl_3$/50 mM sodium citrate (Tb–vesicles); (ii) 50 mM sodium dipicolinate/20 mM NaCl (DPA–vesicles); or (iii) 2.5 mM $TbCl_3$/25 mM sodium citrate/25 mM sodium dipicolinate/10 mM NaCl (Tb/DPA–vesicles). All the above media contained 5 mM Hepes adjusted to a final pH of 7.4. Vesicles were separated from nonencapsulated material by gel filtration on Sephadex G-75 using 100 mM NaCl, 1.0 mM EDTA, and 5 mM Hepes (pH 7.4) as elution buffer.

For the RET assay, 0.6 mol % (relative to lipid phosphorus) each of *N*-NBD-PE and *N*-Rh-PE was incorporated in the vesicle bilayer. Vesicles were prepared in 100 mM NaCl, 0.1 mM EDTA, and 5 mM Hepes (pH 7.4) as described above. Unlabeled vesicles were prepared in the same buffer.

Phospholipid phosphorus was determined according to the method of Bartlett (1959).

Fluorescence Measurements. Mixing of aqueous vesicle contents was measured by using the Tb/DPA assay as described previously (Wilschut et al., 1980, 1981, 1983). A small aliquot (100 μL) of a concentrated 1:1 mixture of Tb– and DPA–vesicles was injected into a cuvette containing a final volume of 2.0 mL of 100 mM NaCl, 0.1 mM EDTA, 5 mM Hepes (final concentrations), and $CaCl_2$ at the desired final concentration. The medium in the cuvette was stirred continuously and maintained at the desired temperature. Fluorescence was recorded continuously by using an SLM 8000 fluorometer equipped with a double excitation monochromator (SLM/Aminco, Urbana, IL). Excitation and emission wavelengths were 276 and 545 nm, respectively, and a cutoff filter (<530 nm) was placed between the sample and the emission monochromator. The fluorescence scale was calibrated such that the 100% value corresponded to all of the Tb present being complexed to DPA (Wilschut et al., 1980, 1981).

Leakage of vesicle contents was measured by following the fluorescence quenching of preencapsulated Tb/DPA complex upon its release into the external medium (Bentz et al., 1983b). Measurements were carried out in the same way as the fusion measurements, except that one population of Tb/DPA–vesicles (at the same total phospholipid concentration as in the corresponding fusion measurements) was used. Calibration of the fluorescence scale was the same as in the corresponding fusion measurements and gave 100% initial fluorescence intensity in each of the release experiments.

The RET assay monitors continuously the relief of energy transfer between *N*-NBD-PE and *N*-Rh-PE as the two probes dilute from a labeled into an unlabeled vesicle bilayer (Struck et al., 1981). The increase of *N*-NBD-PE fluorescence was measured in a 1:1 mixture of labeled and unlabeled vesicles under conditions otherwise identical with those in the Tb/DPA assay. Excitation and emission wavelengths were 465 and 530 nm, respectively, with a cutoff filter (<520 nm) between the sample and the emission monochromator. The fluorescence scale was calibrated such that the zero level corresponded to the initial residual fluorescence of the labeled vesicles and the 100% value to complete mixing of all the lipids in the system. The latter value was set by the fluorescence intensity of vesicles, labeled with 0.3 mol % each of the fluorophores, at the same total lipid concentration as that in the fusion assay. It should be noted that, in the concentration range of the fluorophores used, the *N*-NBD-PE fluorescence intensity increases linearily with the dilution of the probes (Struck et al., 1981).

Theoretical Analysis

Details of the theoretical analysis of vesicle fusion have been presented elsewhere (Nir et al., 1980b, 1982, 1983; Bentz et al., 1983a,b). Briefly, the analysis is based on a mass action kinetic model which describes the fusion process as consisting of two distinct, but kinetically coupled, stages: first, the aggregation of the vesicles and, second, the fusion reaction proper. The aggregation is a second-order process, its rate being dependent on the square of the initial vesicle concentration. On the other hand, the fusion reaction per se is a first-order process. Thus, at low vesicle concentrations, aggregation is slow, and since fusion occurs without any significant delay, the overall process is rate limited by the aggregation step. On the other hand, at higher vesicle concentrations aggregation is relatively fast, and, thus, the fusion step per se starts to become the rate-limiting step.

The first step in the analysis of Tb/DPA consists of correcting the observed Tb fluorescence for the release of vesicle contents. The measurements provide the percent Tb fluorescence, $F(t)$, and the percent dissociation of preencapsulated Tb/DPA complex, $D(t)$. The corrected percent Tb fluorescence, $I(t)$, is given by (Nir et al., 1980b; Bentz et al., 1983a,b)

$$I(t) = F(t) + 0.5D(t) \tag{1}$$

The factor 0.5 in this equation is due to the fact that only 50% of the fused dimers are productive in terms of fluorescence development. At later stages of the fusion process, when fused trimers, tetramers, etc. become more abundant, the correction due to dissocation should be increased, but up to $I(t)$ = 20–25%, the Tb fluorescence is mostly contributed by dimers (Bentz et al., 1983a). In addition, in the initial stages of the fusion process, $D(t)$ is small compared to $F(t)$. Therefore, the above correction is adequate.

Bentz et al. (1983a) obtained the following approximate formula for $I(t)$ during the early stages of fusion in a 1:1 mixture of Tb– and DPA–vesicles:

$$I(t) = 100A(t)\mathcal{F}(t) \tag{2}$$

where

$$A(t) = (1 + 4C_{11}X_0t)^{1/4} - 1 \tag{3}$$

and

$$\mathcal{F}(t) = 1 - [1 - \exp(-f_{11}t)]/f_{11}t \quad (4)$$

In these equations, X_0 is the initial molar concentration of the vesicles, C_{11} ($M^{-1}\cdot s^{-1}$) is the rate constant for vesicle aggregation, and f_{11} (s^{-1}) is the rate constant for the fusion reaction. When $C_{11}X_0 \ll f_{11}$, i.e., when the vesicle concentration is low, the aggregation step is rate limiting, and the value of f_{11} has little effect on the rate of the overall fusion process. Consequently, a sharply defined value of C_{11} can be obtained by fitting the experimental values of $I(t)$ to the model. Next, the value of f_{11} can be determined by fitting the data obtained with a more concentrated vesicle suspension, where $C_{11}X_0$ is of the same order of magnitude as f_{11} and, thus, the fusion step per se determines to a considerable extent the rate of the overall process. In principle, choosing two appropriate vesicle concentrations allows the unambiguous determination of both C_{11} and f_{11}, but the uncertainty of their values is reduced by testing the simulation of the fusion data at other vesicle concentrations as well. In our calculations, we employ only two parameters, C_{11} and f_{11}, and neglect the process of deaggregation of aggregated vesicles. In the Appendix, it is demonstrated that vesicle deaggregation can indeed be ignored in the present experimental system.

In the RET assay, a population of vesicles labeled with *N*-NBD-PE and *N*-Rh-PE is mixed with a population of unlabeled vesicles in a 1:1 ratio. The calculation of the *N*-NBD-PE fluorescence is simple, since in the concentration range used the fluorescence intensity increases linearly with the dilution of the probes (Struck et al., 1981). Let us denote the labeled vesicles by L and the unlabeled ones by B. Combinations in fused dimers then are LL, BL, and BB at relative weights of $^1/_4$, $^1/_2$, and $^1/_4$, respectively. Only LB contributes to the fluorescence development, and its intensity is 100% at the calibration of the fluorescence scale used. Since LB contains 50% of the total amount of *N*-NBD-PE, the increase in fluorescence intensity at the dimer stage is 50%, i.e., the same as the corresponding value in the Tb/DPA assay (Nir et al., 1980b). In the case of fused trimers, the possible combinations are LLL, LLB, LBB, and BBB at relative weights of $^1/_8$, $^3/_8$, $^3/_8$, and $^1/_8$, respectively. Only the mixed trimers, LLB and LBB, contribute to the fluorescence increase. The fluorescence intensity in LLB is 66.7%, while that in LBB is 133.3%. Since LLB and LBB contain 50% and 25% of the total amount of *N*-NBD-PE, respectively, the fluorescence increase at the trimer stage is 66.7%. Accordingly, the fluorescence increase at the tetramer stage is 75%. In the Tb/DPA assay, the corresponding relative fluorescence intensities are slightly higher (75% and 87.5% in the trimer and tetramer stage, respectively; Nir et al., 1980b). However, in the initial stages of the process, up to $I(t) = 20$–25%, where dimer formation is predominant (Bentz et al., 1983a), the difference in $I(t)$ values between the two assays is minimal, and consequently, we have employed eq 2–4 also in the analysis of the RET fusion data.

Results

Lipid Mixing vs. Mixing of Aqueous Contents. Curve a in Figure 1 shows the fluorescence development upon injection of a 1:1 mixture of Tb- and DPA-containing CL/DOPC LUV into a medium containing 11 mM Ca^{2+}. An initial rapid fluorescence increase was observed, followed by a slow decrease. The initial increase is due to mixing of internal contents during vesicle fusion, while the subsequent decrease is due to release of vesicle contents into the external medium, resulting in dissociation of the Tb/DPA complex and quenching of its fluorescence (Wilschut & Papahadjopoulos, 1979; Wilschut et al., 1980, 1981, 1982, 1983).

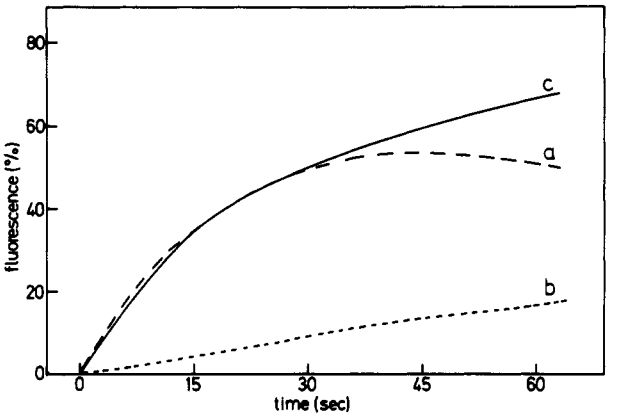

FIGURE 1: Fluorescence development during Ca^{2+}-induced fusion of CL/DOPC LUV at 25 °C monitored with the Tb/DPA assay and the RET assay. (Curve a) A 1:1 mixture of Tb- and DPA-vesicles was injected into a medium containing 11 mM $CaCl_2$ (final concentration); the final total phospholipid phosphorus concentration was 50 μM. The increase of the Tb fluorescence intensity was monitored continuously. (Curve b) Tb/DPA-vesicles were injected into the Ca^{2+}-containing medium to the same final lipid concentration as in (a), and the *decrease* of the fluorescence intensity was monitored continuously. (Curve c) A 1:1 mixture of unlabeled vesicles and vesicles labeled with *N*-NBD-PE and *N*-Rh-PE was injected into the Ca^{2+}-containing medium under conditions otherwise identical with those in (a), and the increase of *N*-NBD-PE fluorescence intensity was monitored.

The rate of release of contents was determined directly in a parallel experiment in which the Tb/DPA complex was encapsulated in the vesicles and the decrease of its fluorescence followed under conditions otherwise identical with those in the fusion assay. The results (Figure 1, curve b) clearly show that the rate of release was considerably slower than that of the mixing of contents (curve a), indicating, in agreement with previous observations (Wilschut et al., 1982), that during the initial stages of the process fusion is largely nonleaky.

Curve c of Figure 1 shows the kinetics of lipid mixing, determined with the RET assay, during the fusion of the vesicles. A 1:1 mixture of CL/DOPC LUV, labeled with *N*-NBD-PE and *N*-Rh-PE, and unlabeled LUV was injected into a medium containing 11 mM Ca^{2+}, and the *N*-NBD-PE fluorescence intensity was monitored continuously. A rapid fluorescence increase was observed, reflecting the dilution of the fluorescent probes from the labeled into the unlabeled vesicles.

As discussed above, the calibration of the fluorescence scales in the Tb/DPA assay and the RET assay was such that the initial fluorescence development in either case can be compared directly. As can be seen in Figure 1, the initial kinetics of lipid mixing and aqueous contents mixing were essentially identical. Due to leakage of vesicle contents and for reasons discussed under Theoretical Analysis, at later stages of the fusion process the results obtained with the two assays can be expected to deviate.

Mass Action Kinetic Analysis. To determine the separate rate constants for vesicle aggregation and fusion, C_{11} and f_{11}, respectively, measurements were carried out at different vesicle concentrations by utilizing both the Tb/DPA assay and the RET assay, at 25 °C and 11 mM Ca^{2+}. Triplicate measurements were done for each of the experimental conditions, and the results agreed to within 1% of the fluorescence scale. Figure 2 shows that the data could be well fitted with the mass action kinetic model. The data points in panel A represent the time course of the percent Tb fluorescence, corrected for

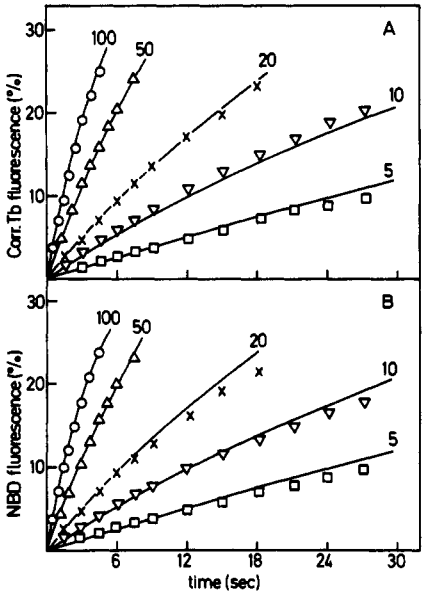

FIGURE 2: Mass action kinetic simulation of Ca^{2+}-induced fusion of CL/DOPC LUV at 25 °C monitored with the Tb/DPA assay (A) and the RET assay (B). Fusion was measured at 11 mM Ca^{2+} in 1:1 mixtures of Tb– and DPA–vesicles (Tb/DPA assay) or labeled and unlabeled vesicles (RET assay) at different vesicle concentrations. Total micromolar phospholipid phosphorus concentrations are indicated. The data points represent the experimental fluorescence intensities (in the case of the Tb/DPA assay, corrected for leakage of vesicle contents) and the drawn lines the theoretical simulation that gave an optimal fit to the data.

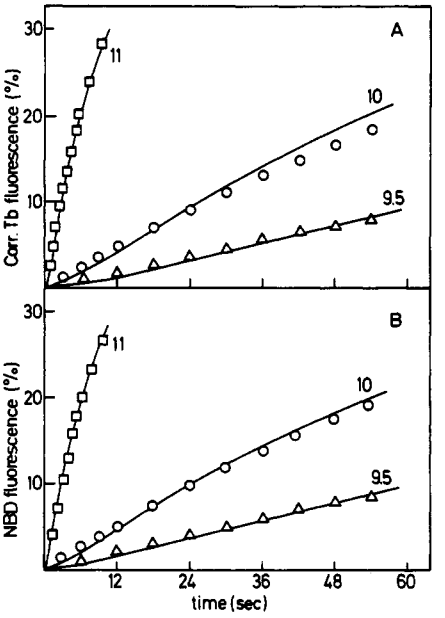

FIGURE 3: Representative examples of mass action kinetic simulation of CL/DOPC LUV fusion at different Ca^{2+} concentrations. Fusion was monitored at 25 °C with the Tb/DPA assay (A) and the RET assay (B), as described in the legends to Figures 1 and 2, at 9.5, 10, and 11 mM Ca^{2+}. The data points represent the experimental fluorescence intensities and the drawn lines the theoretical simulation. Total phospholipid phosphorus concentration in the examples shown was 50 μM.

leakage of vesicle contents, at different vesicle concentrations. The drawn lines represent the theoretical simulation that gave the best fit to the experimental data. The rate constants determining the time course of the process were $C_{11} = 8.0 \times 10^7$ $M^{-1}s^{-1}$ and $f_{11} = 4.0$ s^{-1}. Similarly, the data points in panel B represent the experimental *N*-NBD-PE fluorescence and the drawn lines the simulation. The values of the rate constants that gave an optimal fit in this case were very similar to those obtained with the Tb/DPA assay: $C_{11} = 6.0 \times 10^7$ $M^{-1}s^{-1}$ and $f_{11} = 3.0$ s^{-1}.

Ca^{2+} Dependence of Aggregation and Fusion. The overall rate of fusion of LUV composed of an equimolar mixture of CL and egg phosphatidylcholine has been shown previously to be strongly dependent on the Ca^{2+} concentration in a narrow range (Wilschut et al., 1982). Virtually identical results were obtained now with CL/DOPC LUV, with either the RET assay or the Tb/DPA assay. At Ca^{2+} concentrations below 9 mM, no fluorescence increase was detected, at least on the time scale of the experiment. Above 9 mM, the initial rate of fluorescence development in either assay increased dramatically with increasing Ca^{2+} concentrations (results not shown).

To determine separately the rate of vesicle aggregation and that of the fusion step per se, fusion measurements were carried out at three Ca^{2+} concentrations in the critical range, each at different vesicle concentrations. In each case, the results could be well fitted with the model. Representative examples at one vesicle concentration are shown in Figure 3. Rate constants for aggregation and fusion are summarized in Table I. At each of the Ca^{2+} concentrations, the rate constants obtained with either the Tb/DPA assay or the RET assay were identical within the limits of precision. Remarkably, the aggregation and the fusion rate constants increased with increasing Ca^{2+} concentrations in a parallel fashion (Figure 4A).

Effect of Temperature. To determine the temperature dependence of aggregation and fusion of CL/DOPC LUV at different Ca^{2+} concentrations, we performed the fusion measurements also at 37 °C. Again, a good fit of the data with the model was obtained (results not shown). A summary of rate constants is given in Table I. As can be seen, both aggregation and fusion rate constants were significantly higher at 37 °C than at 25 °C. Interestingly, at 37 °C, fusion rate constants obtained with the RET assay were slightly, but consistently, higher than those obtained with the Tb/DPA assay, while the aggregation rate constants were essentially the same. Similar to 25 °C, the aggregation and fusion rate constants at 37 °C increased with increasing Ca^{2+} concen-

Table I: Ca^{2+}-Induced Aggregation and Fusion of CL/DOPC LUV: Survey of Rate Constants[a]

temp (°C)	Ca^{2+} concn (mM)	aggregation rate constant, C_{11} ($M^{-1}\cdot s^{-1}$)[b]		fusion rate constant, f_{11} (s^{-1})[b]	
		Tb/DPA	RET	Tb/DPA	RET
25	9.5	3.5×10^6	3.6×10^6	0.1	0.17
	10	9.0×10^6	9.0×10^6	0.3	0.4
	11	8.0×10^7	6.0×10^7	4.0	3.0
37	9.5	1.3×10^7	1.9×10^7	0.4	1.5
	10	3.5×10^7	4.6×10^7	1.0	3.0
	11	1.6×10^8	2.0×10^8	10	30

[a] Fusion was measured (as described in the legends to Figures 1 and 2) at 25 and 37 °C at 9.5, 10, and 11 mM Ca^{2+} and at 5, 10, 20, 50, and 100 μM total phospholipid phosphorus. The results were analyzed in terms of the mass action kinetic model, employing a concentration of vesicles of 1.2×10^{-11} M at 1 μM phospholipid phosphorus. This value is based on an area per molecule of 70 $Å^2$ for DOPC and 140 $Å^2$ for CL and a vesicle diameter of 1000 Å. Rate constants corresponding to simulations that gave an optimal fit to the data are presented. [b] The estimated relative uncertainty of the C_{11} values is ±20%, and that of the f_{11} values ±40%. The larger relative uncertainty of the f_{11} values is due to the fact that this parameter is determined primarily by the fusion measurements at the higher vesicle concentrations, where the overall rate of fusion is fast. The C_{11} values are determined by the fusion rates at the lower vesicle concentrations. These rates are relatively slow and, thus, can be measured more accurately (see Theoretical Analysis).

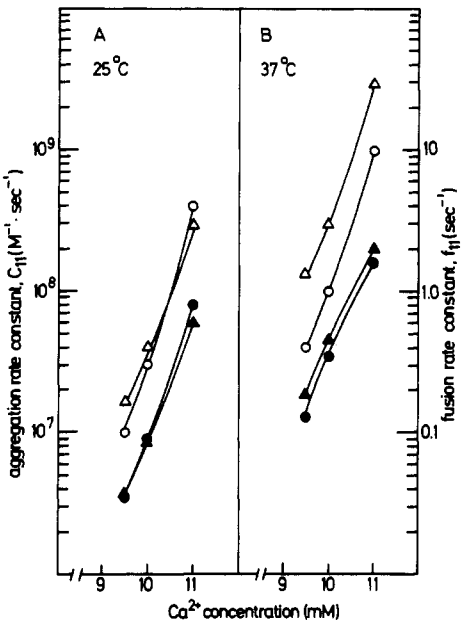

FIGURE 4: Dependence of the aggregation and fusion rate constants on the Ca^{2+} concentration at 25 (A) and 37 °C (B). (Circles) Parameters obtained with the Tb/DPA assay; (triangles) parameters obtained with the RET assay; (closed symbols) aggregation rate constants; (open symbols) fusion rate constants.

trations in a remarkably parallel fashion (Figure 4B).

Discussion

Lipid Mixing vs. Mixing of Aqueous Contents. In this study, we have determined the kinetics of bilayer lipid and aqueous contents mixing during Ca^{2+}-induced fusion of CL/DOPC LUV. The results could be well simulated in terms of a mass action kinetic model, providing separate rate constants for vesicle aggregation and for the fusion reaction per se. The meaning of these parameters can be defined as follows. The aggregation rate constant obtained with the RET assay is proportional to the frequency of formation of vesicle aggregates, resulting in lipid mixing, while that obtained with the Tb/DPA assay reflects the frequency of aggregate formation, resulting in mixing of aqueous contents. The fusion rate constants, on the other hand, reflect the probability that lipid mixing (RET assay) or aqueous contents mixing (Tb/DPA assay) occurs *after* aggregate formation.

In principle, lipid mixing can occur through different mechanisms. First, lipid molecules may be transferred between isolated vesicles through the aqueous phase. Second, lipid transfer may occur during transient vesicle collisions or after vesicle aggregation. Third, lipid mixing may occur as a result of membrane fusion. It has been observed previously that the fluorophores used in the RET assay do not exchange between membrane vesicles through the aqueous medium (Struck et al., 1981; Hoekstra, 1982; Kumar et al., 1982; Nichols & Pagano, 1983). In agreement with these observations, our present results clearly show that lipid mixing is dependent on vesicle aggregation and rule out the possibility of transfer of individual lipid molecules through the aqueous medium. Moreover, since the aggregation rate constants obtained with either assay are essentially the same (Table I), lipid mixing does not occur during transient vesicle collisions but only during vesicle aggregation events that also result in mixing of aqueous vesicle contents.

With respect to the possibility of lipid transfer between aggregated vesicles, the identical fusion rate constants obtained with either assay at 25 °C (Table I) show that at this temperature the probabilities of lipid mixing and aqueous contents mixing, occurring *after* vesicle aggregation, are the same. This indicates that at 25 °C lipid mixing is exclusively the result of membrane fusion. At 37 °C, the fusion rate constants obtained with the RET assay were slightly, but consistently, higher than those obtained with the Tb/DPA assay (Table I). This observation implies that at this temperature the vesicles, once aggregated, have a somewhat higher tendency to mix lipids than to mix aqueous contents. This could be due to a rapid transfer of individual lipid molecules, at this temperature preceding the coalescence of internal vesicle contents. Alternatively, the formation of a fusion intermediate, in which the outer lipid monolayer is continuous but the communication between the internal compartments not yet established, may become distinguishable at higher temperatures. At present, we cannot yet discriminate between these two possibilities.

Ca^{2+} Dependence of Vesicle Aggregation. Bentz & Nir (1981) have shown that the rate constant for aggregation of spherical colloidal particles, such as phospholipid vesicles, can be well estimated by

$$C_{11} = \left[\frac{4kTN_A}{3\eta}(2d^*/R)\right] \exp(-V^*/kT) \times 10^{-3}\ M^{-1}\cdot s^{-1} \quad (5)$$

in which η is the bulk viscosity of the medium, kT the thermal energy of the vesicles, N_A Avogadro's number, and V^* the potential barrier of interaction between two vesicles (each of radius R) separated by a distance d^* where $d^* = 2/\kappa$ in which κ is the reciprocal of the Debye–Hückel length. With decreasing height of the potential barrier, V^*, the rate of vesicle aggregation will increase (Fuchs, 1934; Verweij & Overbeek, 1948).

The results in Table I and Figure 4 show a dramatic increase of the C_{11} values for aggregation of CL/DOPC LUV when the Ca^{2+} concentration in the medium is raised from 9.5 to 11 mM. The relatively low rates of aggregation at 9.5 mM Ca^{2+} indicate that there is still a significant residual potential barrier between the vesicles under these conditions. On the other hand, at 11 mM Ca^{2+}, the aggregation rate constant reached high values (Table I) that were only 1 order of magnitude below the values expected in diffusion-controlled aggregation (Smoluchowski, 1917). As the expression for the rate constant of diffusion-controlled aggregation does not contain the hydrodynamic correction, $2d^*/R$ (Spielman, 1970; Honig et al., 1971), which may amount to a reduction of C_{11} by about 1 order of magnitude, our results imply that at 11 mM Ca^{2+} the residual potential barrier between the vesicles is very small.

A difference in the height of the potential barrier at 9.5 and 11 mM Ca^{2+} is also indicated by the temperature dependence of the aggregation rate constants. The increase of C_{11} with increasing temperature, due to the term $\exp(-V^*/kT)$ in eq 5, is expected to be less significant at smaller values of V^*. Indeed, the results in Table I show that in the presence of 11 mM Ca^{2+} an increase of the temperature from 25 to 37 °C results in only a doubling of the value of C_{11}, whereas at 9.5 mM Ca^{2+} there is a 4-fold increase of C_{11} in the same temperature range.

A reduction of the height of the potential barrier between negatively charged phospholipid vesicles with increasing Ca^{2+} concentrations is expected in view of an enhanced neutralization of the vesicles' surface charge due to Ca^{2+} binding. However, increased charge neutralization cannot possibly be the only explanation for the dramatic enhancement of the aggregation rate constants within the narrow Ca^{2+} concen-

tration range from 9.5 to 11 mM. Since at 6 mM Ca^{2+}, i.e., below the threshold concentration for vesicle aggregation, the molar binding ratio of Ca^{2+} to CL in the outer monolayer of CL/DOPC LUV is already as high as about 0.8 (J. Wilschut, unpublished results), the binding of Ca^{2+} to dispersed vesicles, i.e., in the stage before vesicle aggregation, is expected to increase by less than 1% when the Ca^{2+} concentration is raised from 9.5 to 11 mM. On the basis of mere electrostatic considerations, the corresponding increase of the aggregation rate constant would be maximally 2-fold (Nir & Bentz, 1978; Nir et al., 1978, 1980a, 1983). However, the values of C_{11} at 11 mM Ca^{2+} are larger by more than an order of magnitude than the corresponding C_{11} values at 9.5 mM Ca^{2+} (Table I). As an explanation for this remarkably steep rise of C_{11}, one has to invoke the occurrence of structural changes in the vesicle bilayer, which, in addition to the effect of increased charge neutralization, further lower the potential energy barrier between the vesicles and, thus, enhance the rate of vesicle aggregation. A similar proposal has been raised before (Nir et al., 1980a) to explain the observation that small PS vesicles in the presence of 1.5 mM Ca^{2+} in a low ionic strength medium exhibit a rate of aggregation several orders of magnitude faster than the rate expected on the basis of electrostatic calculations.

Correlation between the Rate Constants for Aggregation and Fusion. An important result of the present study is the finding that with increasing Ca^{2+} concentrations the fusion rate constants of CL/DOPC LUV increase in parallel with the aggregation rate constants (Figure 4). At first glance, this result may seem trivial in the sense that, obviously, the vesicles have to aggregate before they can fuse and that, therefore, the rate of fusion will increase when the rate of aggregation increases. However, it should be emphasized that the fusion rate constant does not reflect the rate of the overall fusion process but rather the tendency of the vesicles to fuse *after* aggregation. Since the aggregation and fusion rate constants are dependent on the Ca^{2+} concentration in a remarkably similar fashion (Figure 4), the two parameters appear to be correlated, which would imply that the tendency of the vesicles to fuse *after* aggregation is determined by their tendency to aggregate. In the previous paragraph, it has been argued that the steep rise of the aggregation rate constant within a limited Ca^{2+} concentration range can only be explained by the occurrence of structural changes in the vesicle bilayer. The correlation between aggregation and fusion rate constants, therefore, suggests that these structural changes in the vesicle bilayer, in addition to facilitating vesicle aggregation, also cause a significant destabilization of the bilayer, rendering the vesicles susceptible to fusion.

At present, the nature of the structural changes in the vesicle bilayer that enhance aggregation and induce fusion remains largely obscure. However, two points can be made. First, since fusion by necessity requires establishment of hydrophobic contact between the apposed bilayer surfaces, the structural changes are likely to involve a disruption of the hydration barrier between the vesicles (Rand, 1981). That such changes would also facilitate the formation of stable vesicle aggregates is quite conceivable, as the major repulsive force between phospholipid bilayers at close distances of separation is due to the strong hydration of the bilayer surfaces (Rand, 1981). Second, the structural changes are likely to be induced by vesicle/vesicle interaction rather than by sole binding of Ca^{2+} to dispersed vesicles. In this respect, it should be noted that, at any concentration below the threshold required for vesicle aggregation, Ca^{2+} fails to induce structural changes in isolated CL/DOPC LUV, resulting in an enhanced permeability of the vesicle bilayer to Ca^{2+} or carboxyfluorescein, even though under these conditions the Ca^{2+}:CL binding ratio in the outer monolayer of the vesicles can be as high as 0.8 (J. Wilschut, unpublished results). It seems unlikely that at slightly higher Ca^{2+} concentrations a small increase of the Ca^{2+}:CL binding ratio would result in drastic bilayer alterations at the level of dispersed vesicles, i.e., in the stage *before* aggregation. On the other hand, a small increase of the Ca^{2+}:CL binding ratio does result in a reduction of the distance of separation between colliding vesicles. Therefore, the structural bilayer alterations are likely to be local events, occurring at the site of closest distance between colliding vesicles. One may speculate that a local change in bilayer curvature occurs which is known to facilitate both aggregation, due to a lowering of the potential energy barrier between the vesicles (Verweij & Overbeek, 1948; Nir et al., 1980b), and fusion, presumably due to constraints in lipid packing (Nir et al., 1982).

Acknowledgments

We thank Dr. Gerrit Scherphof for his interest in the project and Rinske Kuperus for expert secretarial assistance.

Appendix

Estimation of Deaggregation Rate Constants. In this section, we show that in the analysis of Ca^{2+}-induced aggregation and fusion of CL/DOPC LUV, ignoring deaggregation of aggregated vesicles is justified and does not result in a significant uncertainty of the values of C_{11} and f_{11}.

The rate constant, D_{11}, for deaggregation of aggregated vesicles (each of radius R = 50 nm) is given by (Petrucci, 1971; Bentz & Nir, 1981)

$$D_{11} = (4 \times 10^{-7}) C_{11} \exp(-u/kT) \qquad \text{(A1)}$$

in which u is the depth of the potential well holding the particles at close contact and C_{11} now is the *forward* rate of aggregation rather than the net effective rate. Due to the term $\exp(-u/kT)$, D_{11} rises more steeply with increasing temperature than C_{11}. If deaggregation processes would be occurring to a considerable extent, one would expect the observed, effective, value of C_{11} to decrease with increasing temperature. The observation that the effective values of C_{11} (Table I) *increase* with increasing temperature is an indication, therefore, that deaggregation processes can be ignored in the analysis of the fusion data. This does not mean that $D_{11} = 0$ but rather than the rate of deaggregation is small compared to the rate of fusion, i.e., $D_{11} \ll f_{11}$.

It has been shown by Bentz et al. (1983a) that the effective values of C_{11} and f_{11} (denoted in the following by $\hat{C}_{11}$ and $\hat{f}_{11}$), i.e., the values found by fitting the data employing eq 2–4 which ignore reversibility of aggregation, are related to their true values, C_{11} and f_{11}, by

$$\hat{C}_{11} = C_{11}/(1 + D_{11}/f_{11}) \qquad \text{(A2)}$$

and

$$\hat{f}_{11} = f_{11} + D_{11} \qquad \text{(A3a)}$$

or

$$D_{11} = \hat{f}_{11} - f_{11} < \hat{f}_{11} \qquad \text{(A3b)}$$

Hence, from the parameters obtained with the Tb/DPA assay (Table I), we deduce that D_{11}(37 °C, 9.5 mM Ca^{2+}) < 0.4 s^{-1}. From this value at 9.5 mM Ca^{2+}, we can now deduce that vesicle deaggregation can be ignored at 11 mM Ca^{2+}. In order to show how this conclusion is reached, we choose a value of D_{11}(37 °C, 9.5 mM Ca^{2+}) lower than 0.4 s^{-1}, for example, 0.2 s^{-1} (the choice of another value, like 0.3 or 0.1 s^{-1}, yields a

similar conclusion). Hence, $D_{11} = 0.2 = (4 \times 10^{-7})C_{11}(37\ °C, 9.5\ mM\ Ca^{2+})\ \exp(-u/kT) = 2(4 \times 10^{-7})(1.3 \times 10^{7}) \times \exp(-u/kT)$, since from eq A2 and A3a we deduce that $C_{11} = 2\hat{C}_{11}$. This relationship gives $\exp(-u/kT) = 0.02$ at 37 °C and 9.5 mM Ca^{2+}. In the presence of 11 mM Ca^{2+}, u must be larger than or at least equal to its value at 9.5 mM Ca^{2+}, such that $D_{11}(37\ °C, 11\ mM\ Ca^{2+}) < (4 \times 10^{-7})C_{11}(37\ °C, 11\ mM\ Ca^{2+})0.02 < (8 \times 10^{-9})C_{11}(37\ °C, 11\ mM\ Ca^{2+})$. If we take the value for C_{11} equal to $\hat{C}_{11}$ (i.e., $1.6 \times 10^{8}\ M^{-1}\cdot s^{-1}$; Table I), we obtain $D_{11} < 1.3\ s^{-1}$. If we use an extremely large value for C_{11}, we arrive at a chain of inequalities, which eventually gives the same result. For example, $C_{11} = 10^{9}\ M^{-1}\cdot s^{-1}$ would give in the first stage $D_{11} < 8\ s^{-1}$ and $f_{11} > 12\ s^{-1}$, i.e., $D_{11}/f_{11} < {}^{2}/_{3}$ and $C_{11} < {}^{5}/_{3}\hat{C}_{11}$. In the second stage, it would follow that $D_{11} < 2.5\ s^{-1}$ etc.

The upper bound to $D_{11}(37\ °C, 11\ mM\ Ca^{2+})$ of $1.3\ s^{-1}$, deduced above, is much smaller than the corresponding value of f_{11} ($10\ s^{-1}$, Table I), indicating that, indeed, vesicle deaggregation can be ignored. Consistently, if we take a value for $D_{11}(37\ °C, 11\ mM\ Ca^{2+})$ larger than $1.3\ s^{-1}$, we arrive at a contradication of the form $D_{11}(37\ °C, 9.5\ mM\ Ca^{2+}) > \hat{f}_{11}(37\ °C, 9.5\ mM\ Ca^{2+})$. From the above upper bound to D_{11} at 37 °C, an upper bound for D_{11} at 25 °C is obtained since D_{11} decreases with decreasing temperature.

Registry No. DOPC, 4235-95-4; Ca, 7440-70-2.

REFERENCES

Bartlett, G. R. (1959) *J. Biol. Chem. 234*, 466–468.

Bentz, J., & Nir, S. (1981) *Proc. Natl. Acad. Sci. U.S.A. 78*, 1634–1637.

Bentz, J., Nir, S., & Wilschut, J. (1983a) *Colloids Surf. 6*, 333–363.

Bentz, J., Düzgünes, N., & Nir, S. (1983b) *Biochemistry 22*, 3320–3330.

Düzgünes, N., Wilschut, J., Fraley, R., & Papahadjopoulos, D. (1981a) *Biochim. Biophys. Acta 642*, 182–195.

Düzgünes, N., Nir, S., Wilschut, J., Bentz, J., Newton, C., Portis, A., & Papahadjopoulos, D. (1981b) *J. Membr. Biol. 59*, 115–125.

Düzgünes, N., Paiement, J., Freeman, K. B., Lopez, N., Wilschut, J., & Papahadjopoulos, D. (1984) *Biochemistry 23*, 3486–3494.

Fuchs, N. (1934) *Z. Phys. 89*, 736–743.

Hoekstra, D. (1982) *Biochemistry 21*, 2833–2840.

Honig, E. P., Roebersen, G. J., & Wiersema, P. H. (1971) *J. Colloid Interface Sci. 36*, 97–109.

Kumar, N., Blumenthal, R., Henkart, M., Weinstein, J. N., & Klausner, R. D. (1982) *J. Biol. Chem. 257*, 15137–15144.

Nichols, J. W., & Pagano, R. E. (1983) *J. Biol. Chem. 258*, 5368–5371.

Nir, S., & Bentz, J. (1978) *J. Colloid Interface Sci. 65*, 399–414.

Nir, S., Newton, C., & Papahadjopoulos, D. (1978) *Bioelectrochem. Bioenerg. 5*, 116–133.

Nir, S., Bentz, J., & Portis, A. (1980a) *Adv. Chem. Ser. No. 188*, 75–106.

Nir, S., Bentz, J., & Wilschut, J. (1980b) *Biochemistry 19*, 6030–6036.

Nir, S., Wilschut, J., & Bentz, J. (1982) *Biochim. Biophys. Acta 688*, 275–278.

Nir, S., Bentz, J., Wilschut, J., & Düzgünes, N. (1983) *Prog. Surf. Sci. 13*, 1–124.

Olson, F., Hunt, C. A., Szoka, F. C., Vail, W. J., & Papahadjopoulos, D. (1979) *Biochim. Biophys. Acta 557*, 9–23.

Papahadjopoulos, D., Vail, W. J., Newton, C., Nir, S., Jacobson, K., Poste, G., & Lazo, R. (1977) *Biochim. Biophys. Acta 465*, 579–598.

Papahadjopoulos, D., Poste, G., & Vail, W. J. (1979) *Methods Membr. Biol. 10*, 1–121.

Petrucci, S. (1971) in *Ionic Interactions* (Petrucci, S., Ed.) Vol. 2, pp 101–106, Academic Press, New York.

Portis, A., Newton, C., Pangborn, W., & Papahadjopoulos, D. (1979) *Biochemistry 18*, 780–790.

Rand, R. P. (1981) *Annu. Rev. Biophys. Bioeng. 10*, 277–314.

Smoluchowski, M. (1917) *Z. Phys. Chem., Abt. A 92*, 129–168.

Spielman, L. A. (1970) *J. Colloid Interface Sci. 33*, 562–571.

Struck, D. K., Hoekstra, D., & Pagano, R. E. (1981) *Biochemistry 20*, 4093–4099.

Sundler, R., & Papahadjopoulos, D. (1981) *Biochim. Biophys. Acta 649*, 743–750.

Sundler, R., Düzgünes, N., & Papahadjopoulos, D. (1981) *Biochim. Biophys. Acta 649*, 751–758.

Szoka, F. C., & Papahadjopoulos, D. (1978) *Proc. Natl. Acad. Sci. U.S.A. 75*, 4194–4198.

Verwey, E. J., & Overbeek, J. Th. G. (1978) *Theory of the Stability of Lyophobic Colloids*, Elsevier, Amsterdam.

Wilschut, J., & Papahadjopoulos, D. (1979) *Nature (London) 281*, 690–692.

Wilschut, J., & Hoekstra, D. (1984) *Trends Biochem. Sci. (Pers. Ed.) 9*, 479–483.

Wilschut, J., Düzgünes, N., Fraley, R., & Papahadjopoulos, D. (1980) *Biochemistry 19*, 6011–6021.

Wilschut, J., Düzgünes, N., & Papahadjopoulos, D. (1981) *Biochemistry 20*, 3126–3133.

Wilschut, J., Holsappel, M., & Jansen, R. (1982) *Biochim. Biophys. Acta 690*, 297–301.

Wilschut, J., Düzgünes, N., Hong, K., Hoekstra, D., & Papahadjopoulos, D. (1983) *Biochim. Biophys. Acta 734*, 309–318.